Ground-based detection of sodium in the transmission spectrum of exoplanet HD209458b

Snellen I.A.G., Albrecht S., de Mooij E.J.W. and Le Poole R.S.

Leiden Observatory, Leiden University, Postbus 9513, 2300 RA, Leiden, The Netherlands

ABSTRACT

Context. The first detection of an atmosphere around an extrasolar planet was presented by Charbonneau and collaborators in 2002. In the optical transmission spectrum of the transiting exoplanet HD209458b, an absorption signal from sodium was measured at a level of 0.023±0.006%, using the STIS spectrograph on the Hubble Space Telescope. Despite several attempts, so far only upper limits to the Na D absorption have been obtained using telescopes from the ground, and the HST result has yet to be confirmed.
Aims. The aims of this paper are to re-analyse data taken with the High Dispersion Spectrograph on the Subaru telescope, to correct for systematic effects dominating the data quality, and to improve on previous results presented in the literature.
Methods. The data reduction process was altered in several places, most importantly allowing for small shifts in the wavelength solution. The relative depth of all lines in the spectra, including the two sodium D lines, are found to correlate strongly with the continuum count level in the spectra. These variations are attributed to non-linearity effects in the CCDs. After removal of this empirical relation the uncertainties in the line depths are only a fraction above that expected from photon statistics.
Results. The sodium absorption due to the planet's atmosphere is detected at >5σ, at a level of 0.056±0.007% (2×3.0Å band), 0.070±0.011% (2×1.5 Å band), and 0.135±0.017% (2×0.75Å band). There is no evidence that the planetary absorption signal is shifted with respect to the stellar absorption, as recently claimed for HD189733b.
Conclusions. The STIS/HST measurements are confirmed. The measurements of the Na D absorption in the two most narrow bands indicate that some signal is being resolved. Due to variations in the instrumental resolution and intrinsic variations in the stellar lines due to the Rossiter-McLauglin effect, it will be challenging to probe the planetary absorption on spectral scales smaller than the stellar absorption using conventional transmission spectroscopy.

Key words. techniques: spectroscopic – stars: atmosphere – stars: planetary systems

1. Introduction

Transiting extrasolar planets are of great scientific value. While the radial velocity method continues to be very successful in finding planets and characterising their orbits, only transits can currently reveal the properties of the planets themselves. In addition to the basic planetary parameters that can be determined, such as planet mass, size, and average density, the atmospheres of transiting planets can be probed through either secondary eclipse observations (e.g. Charbonneau et al. 2005; Deming et al. 2005; Knutson et al. 2007) or atmospheric transmission spectroscopy, the subject of this paper. In transmission spectroscopy, the depth of a planet transit is measured as function of wavelength. It is expected that at certain wavelengths, a transit will be slightly deeper due to absorption in the planet's atmosphere. In the optical transmission spectrum of hot Jupiters, the strongest of these absorption features was predicted to come from the sodium D lines at 5889 and 5896 Å (Brown 2001; Seager & Sasselov 2000). Indeed, Charbonneau et al. (2002) detected Na D absorption in the transmission spectrum of the transiting exoplanet HD209458b, at a level of 0.023±0.006% in a 12Å wide band, using the STIS spectrograph on the Hubble Space Telescope (HST). This constitutes the first detection of an atmosphere around an extrasolar planet. Subsequently, strong absorption features have been detected in HD209458b from hydrogen, oxygen, and carbon at a level of 5-15%, thought to be caused by an evaporating exosphere (Vidal-Madjar et al. 2003; 2004). Recently,

hot hydrogen has been detected by Ballester et al. (2007), also using HST data. A claim by Tinetti et al. (2007) of the detection of water vapour from a comparison of transit depths at several wavelengths in the infrared, as measured with Spitzer, has been disputed by Ehrenreich et al. (2007). This, while Swain et al. (2008) identify both water and methane from NICMOS/HST data.

Despite several attempts from ground-based observatories, no confirmation has yet been obtained of the Na D planetary absorption feature in the transmission spectrum of HD209458b. In general, ground-based transmission spectroscopy has not been a great success. Typically, upper limits to a Na D absorption signal of 0.1−1% have been reached (Moutou et al. 2001; Snellen 2004; Narita et al. 2005), implying that systematic effects dominate the error budgets. A modern Echelle spectrograph on a 8−10 m. class telescope can provide spectra from the brightest transiting exoplanet systems with signal-to-noise ratios, SNR>100, within a few minutes of exposure time. Integrating over a few Angstrom and over the duration of a transit, this would mean that photon noise statistics should allow detections down to a few times 10^{-4}. Although the HST detection of the Na D absorption feature is only just at this level, it is expected that its width is only a fraction of the 12Å passband used by Charbonneau et al. (2002), as recently shown by re-analysis of the STIS data (Sing et al. 2008). This means that the Na absorption within a 2-3Å band should be at the ∼ 10^{-3} level.

In this paper we re-analyse a data-set from the High Dispersion Spectrograph on the Subaru telescope, that covers
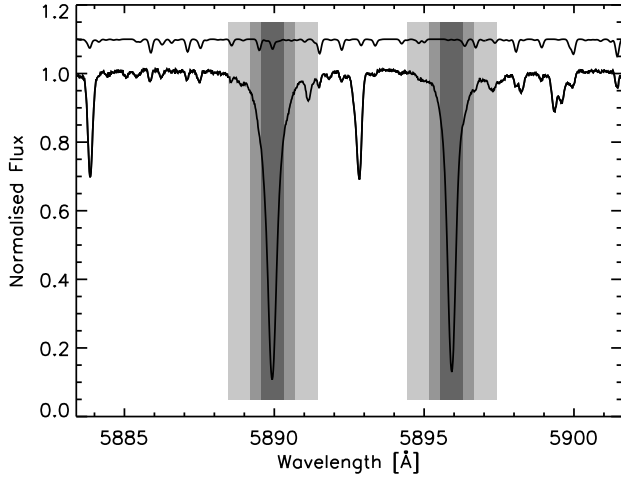
Fig. 1. Spectrum of HD209458 around the Na D doublet. The shaded areas indicate the narrow, medium, and wide passbands as used in our analysis. In all cases, the comparison bands are located directly adjacent to the central band, and have the same width. The upper line shows a synthetic telluric spectrum constructed from the line list of Lundstrom et al. (1991). Note that the telluric sodium absorption can show strong seasonable variability.

Fig. 2. Variations of observing conditions over the 30 spectra. The solid line indicates the airmass, and the dotted line shows the normalised variation in continuum count level. The dashed line indicates the seeing (in σ) as measured from the one-dimensional profile of the star along the slit. The crosses show the relative telluric line strength as measured using strong lines in the red part of the spectrum. It follows the airmass well, implying that the conditions were excellent. The grey band indicates the timing of the planetary transit and periods of ingress and egress.

one transit of HD209458b. The aim is to identify and correct for possible systematic effects, and to improve on the results previously presented by Narita et al. (2005; NAR05). Their analysis resulted in spectra with an SNR of a few hundred in the stellar continuum. However, near strong absorption lines, such as the Na D doublet, clear coherent structures were visible (Figure 2 in NAR05), well in excess of the photon shot noise. While NAR05 argued that the positions of the spectral lines are stable to within 0.01Å, spectral shifts at only a fraction of this level (e.g. due to slit-centering variations) could cause these effects. This encouraged us to analyse this data again. In Section 2, the observations, data reduction and analysis are described. The result on the Na D absorption are presented and discussed in Section 3, together with a comparison with the STIS/HST results, and with a recent detection of Na D absorption in exoplanet HD189733b (Redfield et al. 2008)

2. Observations, data reduction, and analysis

HD209458 was observed on the night of October 24, 2002, using the High Dispersion Spectrograph (HDS; Noguchi et al. 2002) on the Subaru telescope. We obtained the data using the SMOKA archive system (Baba et al. 2002). The observations have been described in Winn et al. (2004) and Narita et al.(2005; NAR05). Thirty-two spectra were taken in *Yb mode* (without the iodine cell), of which the last thirty were made with an exposure time of 500 seconds. The entrance slit was 4″ long and 0.8″ wide, oriented with a constant position angle, resulting in a spectral resolution of R~45 000 with 0.9 km s^{-1} per pixel. We concentrated on the data from the red CCD, which contains 21 orders of 4100 pixels covering 5500Å< λ <6800Å. Twelve of the thirty spectra fall outside the transit (nine before ingress and three after egress), and eighteen during the transit. The uncertainty in the transit timing is neglegible.
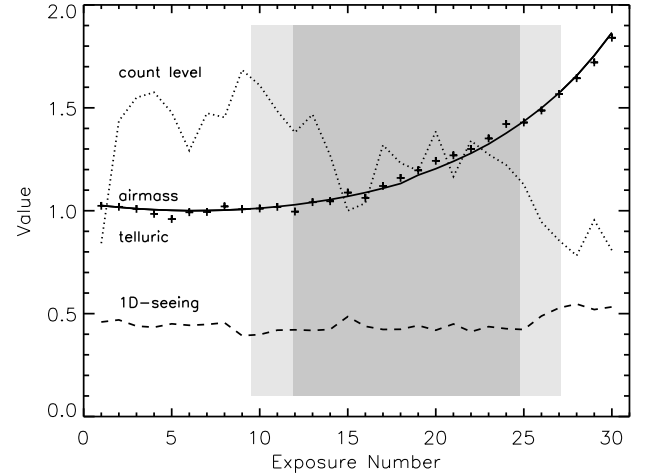
For the initial data reduction we followed the procedure of NAR05. First the frames were processed using the IRAF software package, including the extraction of the one-dimensional spectra. These spectra have signal-to-noise ratios that vary between 300 and 450 per pixel in the continuum. Subsequent analyses were conducted using custom-built procedures in the Interactive Data Language (IDL). Winn et al. (2004) and NAR05 describe a good method to correct for time-dependent variations of the instrumental blaze function (possibly caused by flexure of the spectrograph) using the adjacent orders, which we also use here. We do not apply a global wavelength solution to the spectra. Only for the analysis of the strength of telluric absorption features (see below) did we apply the wavelength solution to the order containing the Na D doublet. The Na D spectral surroundings of HD209458 are shown in Figure 1.

The variations in observing conditions during the night are shown in Fig. 2. The solid line indicates the variation in airmass, and the dashed line the variation in the 1-dimensional stellar profile along the slit (a measure of the seeing). The dotted line shows the normalised variation in continuum count level in the spectra, indicating that it varies up to a factor of two from spectrum to spectrum.

We subsequently selected 59 strong stellar lines and the Na D doublet to perform our analysis. First, for each line, the line center, λ_0, was determined through Gaussian fitting. Subsequently, the total flux was integrated within a spectral band, $\Delta\lambda$, and divided by the average of two equally wide bands to the left and right of the line.

$$
\left.
\begin{aligned}
F_{\mathrm{mid}} &= \int_{\lambda_0-\frac{1}{2}\Delta\lambda}^{\lambda_0+\frac{1}{2}\Delta\lambda} F(\lambda)d\lambda \\
F_{\mathrm{left}} &= \int_{\lambda_0-\frac{3}{2}\Delta\lambda}^{\lambda_0-\frac{1}{2}\Delta\lambda} F(\lambda)d\lambda \\
F_{\mathrm{right}} &= \int_{\lambda_0+\frac{1}{2}\Delta\lambda}^{\lambda_0+\frac{3}{2}\Delta\lambda} F(\lambda)d\lambda
\end{aligned}
\right\}
\qquad
F_{\mathrm{line}} = \frac{2F_{\mathrm{mid}}}{F_{\mathrm{left}} + F_{\mathrm{right}}}
\qquad (1)
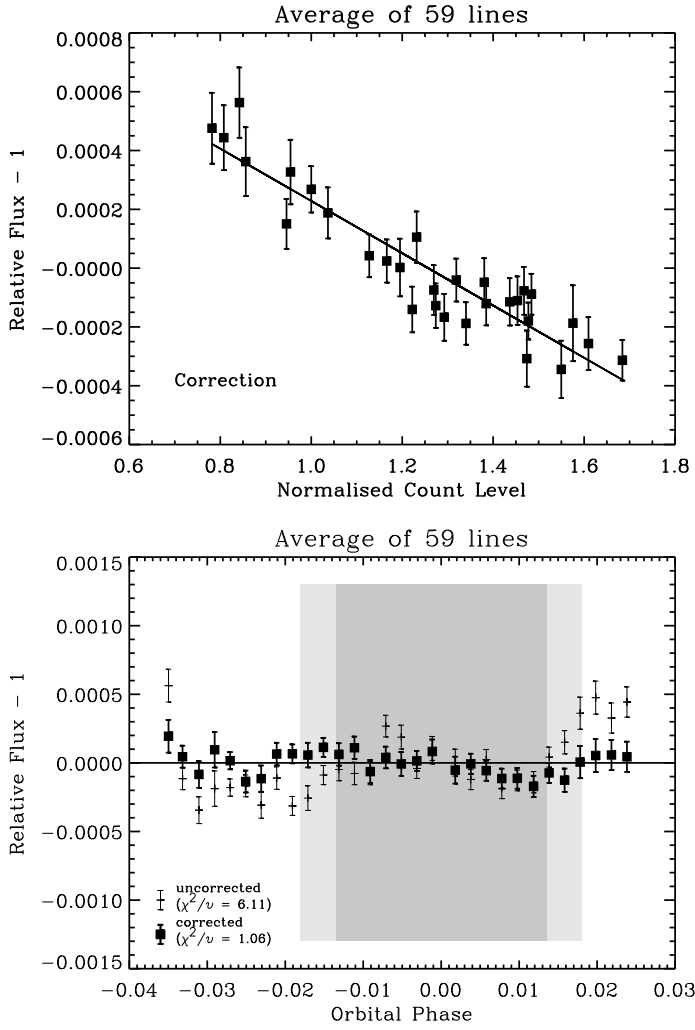$$

Average of 59 lines

Average of 59 lines

Fig. 3. The top panel shows the normalized count level of the continuum in the spectra versus the measured weighted mean-strength of 59 deep stellar absorption lines. A strong inverse correlation is present, with the more flux in the spectra, the deeper the absorption lines. We believe that this is due to a non-linearity effect in the CCD. The solid line indicates the linear least squares fit to the correlation, used to correct the measured line strengths. The lower panel shows the same average strength of these 59 absorption lines as function of orbital phase, where the grey band indicates the planetary transit. Those data points corrected for the correlation with count level (thick squares) have a reduced chi-squared of 1.06, while the uncorrected data exhibit a reduced chi-squared of 6.11.

Subsequently, the relative flux in each line is divided by its average value on the night. Three spectral widths were used of 42, 84 and 166 pixels wide, corresponding to $\Delta\lambda = 0.75$ Å, 1.5 Å, and 3.0 Å, respectively, at the Na D doublet.

2.1. Systematic effects

The variations from spectrum to spectrum, away from spectral lines, are, as expected, dominated by photon noise. However, at and around strong lines, systematic effects play a role. This is in addition to the fact that the signal-to-noise ratios in the cores of deep lines are significantly lower. Most importantly, it was no-

ticed that the observed depths of the Na D lines are a clear function of the overall count level in the spectra. The same effect is visible in the average of the 59 reference lines. In the top panel of Fig. 3, for each spectrum, the normalised continuum level is plotted against the weighted (by line-strength) mean depth of the lines. It shows that the higher the count levels in the spectra, the deeper the lines. Firstly, we convinced ourselves that this is not due to scattered light residuals. It would need about 300 counts per spectral bin to cause this effect, two orders of magnitude above the uncertainties in the scattered light removal. Instead, several other possible causes are identified, but we believe that non-linearity of the CCD is the most likely cause. Other potential systematic effects are caused by variations in the seeing and/or spectral resolution, and intrinsic variations of the stellar spectral line due to the Rossiter-McLaughlin effect (Rossiter 1924). The latter two effects result in strong variations across deep spectral lines, making atmospheric transmission spectroscopy very challenging at spectral scales shorter than the width of the stellar lines.

1 **Non-linearity of the CCD:** Most CCD arrays show low level non-linearity effects, meaning that the conversion factor between electrons and data numbers (ADU) is not constant, but is slowly varying as function of the count-level in a pixel. At levels below the half full well, the conversion factor often decreases towards higher count levels. By assuming a completely linear CCD with constant gain, high count levels are over-estimated, and low count levels (such as in the center of strong absorption lines) are relatively under-estimated. This will make stellar lines appear deeper in those spectra that are better exposed, just as is seen in Fig. 3. Note that the first of the thirty frames was exposed for only 300 sec instead of 500 sec. The lines in this spectrum also follow the relation between line depth and count level. This is in agreement with a non-linearity effect. Unfortunately, to our knowledge, the non-linearity has not been measured for the HDS CCDs. We also found that subtle changes in the order profiles from exposure to exposure makes it impossible to estimate the non-linearity for the CCDs from the flat field exposures. Our tests with a model for the non-linearity of the CCD indicates that a decrease in gain of the order of 2-3% towards 10 000 ADU would be sufficient to explain the effect seen in Fig. 3. By adjusting the raw ADU count levels to $F_{\mathrm{cor}} = (1.0 - 0.03 \times F_{\mathrm{raw}}/10^4)F_{\mathrm{raw}}$ before the reduction process, the effect is largely removed. Note that this is within the range of non-linearity effects seen in other EEV42-80 type CCDs [1].

2 **Variations in spectral resolution and seeing.** Variations in the spectral resolution will also result in variations in the depth of stellar lines. The equivalent width of a line should not vary with spectral resolution, meaning that the difference between two spectra with different spectral resolutions should always integrate to zero over a line. However, the ratio of the two spectra can show strong variations across a line, e.g. because in one of the spectra the line appears much deeper and sharper than in the other spectrum. The latter does not integrate to zero, in particular for very strong lines such as the Na D doublet. Since the HDS is a slit-spectrograph, the seeing influences the exact spectral resolution, and therefore this effect could be present. If the seeing is significantly larger than the slit width, the star light is homogeneously distributed across the slit. If the seeing is

---

[1] e.g. the CCDs of the Wide Field Camera on the Isaac Newton Telescope: http://www.ast.cam.ac.uk/~wfcsur/technical/foibles/

similar to the slit width, or smaller, the light distribution will be peaked, resulting in a higher spectral resolution. This is also the reason why in general slit-spectrographs do not offer the highest stability for radial velocity measurements.

3 **Intrinsic variations of the stellar lines** During the transit, the intrinsic shapes of the stellar lines also change due to the Rossiter-McLauglin effect (Rossiter 1924). When the planet disk crosses the star, it first blocks off part of the stellar surface that due to the star's rotation is moving towards us, and later blocks part of the stellar surface that is moving away from us. This not only results in a radial velocity abberation, but also alters the overall spectral line shape. As above, the equivalent widths of the lines do not change, but the ratio of spectra taken during and outside the transit will show features that do not integrate down to zero.

Changes in the spectral resolution are unavoidable in slit-spectrographs such as the HDS, but should be largely absent in fiber-fed spectrographs. However, the intrinsic variations due to the Rossiter-McLauglin effect will be present in all transmission spectroscopy observations. To avoid the consequences of line shape changes the flux first should be integrated over the total width of the line before it can be compared between spectra, meaning that $\Delta\lambda$ in equation 1 should be large enough. We therefore do our analysis with a minimum width of 0.75 Å.

Most likely, the non-linearity of the pixels in the HDS CCD is causing the effect seen in the top panel of Fig. 3. Since it was not possible to directly measure the non-linearity of the CCD, we corrected for it in an empirical way, by performing a least-squares fit to the correlation between line depth and count level. For the weighted mean of the 59 strong comparison lines, the reduced chi-squared drops from χ^2/ν=6.11 to χ^2/ν=1.05 after this correction. The bottom panel of Fig. 3 shows the remaining residuals. Although there is some correlated variation still visible, it averages out over the transit. Since we integrate over the total extent of the lines, we do not expect variations in the seeing to affect our results. Nevertheless, since the seeing influences how much flux of the star enters the slit, the seeing is anti-correlated with the count level in the spectra. Therefore, a correlation between the seeing and the average line strength is also present. However, the resulting reduced chi-squared is χ^2/ν=2.90, significantly higher than that resulting from the continuum count level, indicating that changes in seeing are not the underlying cause of the line variations.

2.2. The Na D lines and telluric contamination

In a similar manner as for the weighted mean of the reference lines, the correlation between line depth and continuum count level was removed for the Na D doublet. We subsequently determined the depth of the transit for the three Na D passbands separately. A least-squares fit was performed on the data using as a model a scaled version of the HST light curve as presented by Brown et al. (2001). The best fitting model is subsequently removed from the data, revealing low-level variations due to changing telluric contaminations most evident at the end of the night. This telluric residual was found to scale with the airmass and with the strength of some strong telluric lines in the red part of the spectrum (as shown in Fig. 2). A linear fit was performed between the average strength of the strong telluric lines and the Na D residuals to remove the telluric contribution. Note that the fitting of the continuum count level, transit signal, and telluric contamination was performed in a iterative way, but the solutions did not significantly change after the first round.

In addition, a consistency check was performed to see whether our telluric line contamination removal was reasonable. Many telluric lines are present around the Na D doublet, in both the line and reference bands. We used the telluric line list of Lundstrom (1991) to construct a synthetic telluric spectrum. We then constructed a reference spectrum from the average of all exposures which was subsequently removed from the 30 frames. Although the absolute telluric contamination is now lost, all information on the change in telluric contamination becomes clearly visible in this way. The synthetic telluric spectrum was then fitted to these frames, and the change in telluric contribution in the various spectral bands determined. This gives very similar results as the method described above. We use the former method in our final analysis since the contribution of telluric sodium relative to that of water and oxygen undergoes seasonal variations, but within one night is expected to vary following the other telluric lines. Note that NAR05 used the spectrum of the rapidly rotating B5 star HD42545 to remove the telluric contamination around the Na D doublet, however the sodium absoption towards this star is dominated by interstellar contributions (although this is unlikely to have influenced their results).

3. Results and discussion

We measured the depth of the Na D features in the transmission spectrum within three spectral passbands centered on the two stellar lines, with widths of 0.75Å, 1.5Å, and 3.0Å. The results are presented in Fig. 4. The sodium absorption due to the planet's atmosphere is detected at $>5\sigma$, at a level of 0.056±0.007% (2×3Å band), 0.070±0.011% (2×1.5Å band), and 0.135±0.017% (2×0.75Å band). The quoted uncertainties are 1σ error intervals as determined from the SNR in the spectra using chi-square analysis. The resulting reduced chi-squares values, χ^2/ν, are 47/28=1.63, 31/28=1.10, and 45/28=1.75 respectively, and indicate that the residual noise levels are 10−30% higher than expected from Poisson statistics. A way to take this residual noise into account in the error budget is to scale the error bars up such that χ^2/ν=1. This would increase the uncertainties by 10−30%, resulting in conservative estimates of the significance of the sodium detection of $\sim6\sigma$ in each individual passband.

A crucial part of our data analysis is the empirical correction for the correlation of line depth with the continuum count level in the spectra, attributed to non-linearity effects in the CCD. To assess the robustness of our result we performed a slightly different empirical correction by directly correlating the weighted mean-strength of the 59 reference lines with that of the Na D lines. Depending on the passband, this alternative analysis results in a transit depth 20−30% lower than determined above, also with 20-30% higher χ^2/ν values. Since this would still be $\sim5\sigma$ detections, it further supports the detection. Since the first method gives significantly less noisy results, we believe that method it is more reliable.

In our analysis we do not take into account the variation in radial velocity of the planet (and its atmospheric absorption) relative to that of the star. During the transit, the radial velocity of the planet varies from about −14 to +14 km sec^{-1}. For a Lorentzian shaped planetary absorption profile with a width comparable to that of the star (see below), the strength of the absorption signal will have been underestimated by $\sim4\%$ in the narrowest passband. Therefore this is just a minor effect.
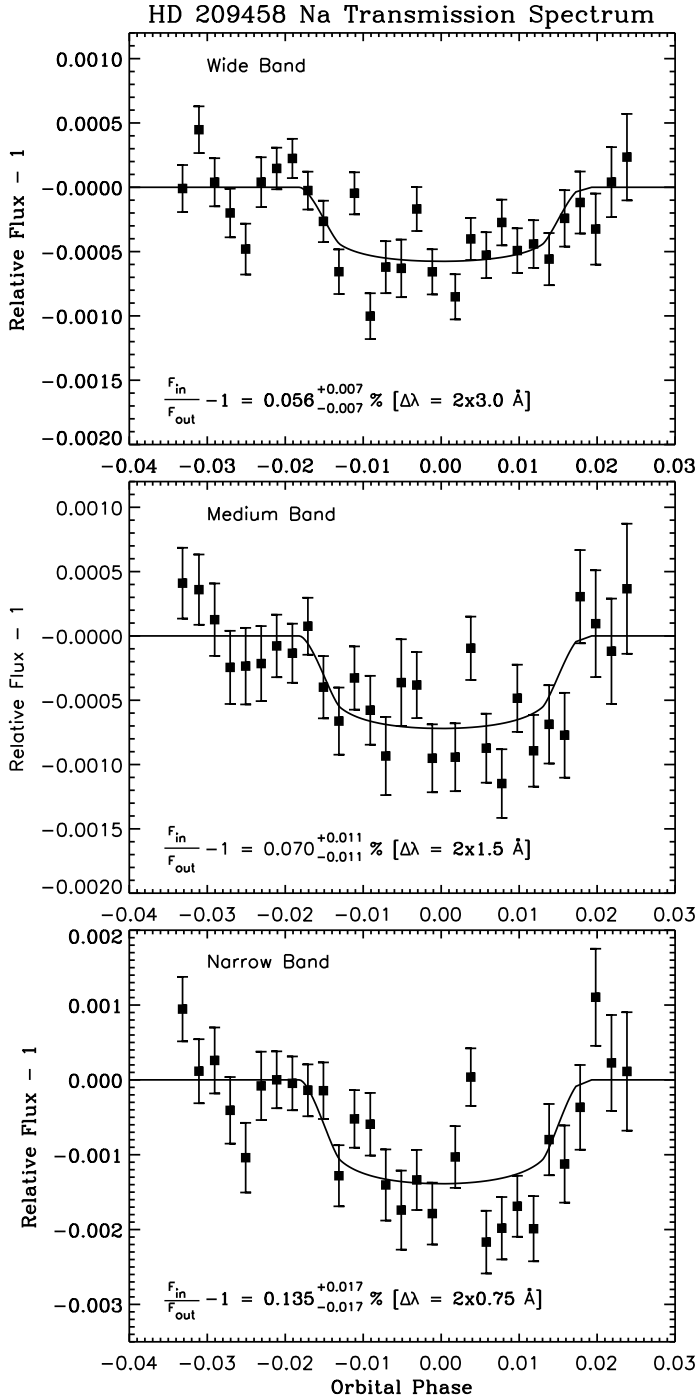
HD 209458 Na Transmission Spectrum

Fig. 4. Transit photometry averaged in two bands centered on the Na D doublet, with spectral widths of 3Å (top panel), 1.5 Å (middle panel) and 0.75 Å (bottom panel). The data have been empirically corrected for the dependence of the depth of stellar lines on the count level in the spectra, as discussed in detail in section 2.1.

HD 209458b Na Absorption

Fig. 5. The three measurements of the Na D absorption in the transmission spectrum of HD209458b in passbands of 2×0.75Å, 2×1.5Å, and 2×3.0Å. The solid line and grey band indicate the HST measurement by Charbonneau et al. (2002) assuming it is completely unresolved and within our passbands. The three dotted lines, indicated by *a, b, c*, are the Na D absorption levels as a function of passband expected from the HST measurements, assuming that the atmospheric absorption feature is Lorentzian shaped with a width equal to, 2×, and 4× the stellar width of the Na D doublet. The two crosses at 4.4 and 9 Å are the results from the re-analysed STIS/HST data by Sing et al. (2008a).

3.1. Comparison with the STIS/HST results

Our results are in excellent agreement with the STIS/HST results presented by Charbonneau et al. (2002) and Sing et al. (2008a). Fig. 5 shows our three measurements of the planetary Na D absorption as a function of the spectral passband. The solid line and gr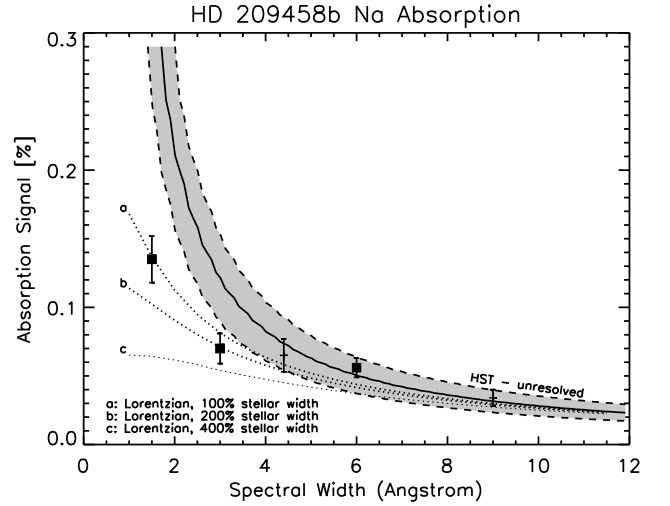ey band shows the STIS/HST result and its uncertainty corrected to our passbands, assuming that the planetary absorption is unresolved and completely within them. If there were no *stellar* Na D lines, then the expected absorption strength as a function of passband would simply scale as $\Delta\lambda^{-1}$. However, since most absorption occurs near the cores of the stellar Na D doublet, where there is already little flux present, the relative contribution of the absorbed part of the spectrum varies more steeply than as $1/\Delta\lambda$. Our measurement in the widest passband is perfectly consitent with an unresolved HST absorption, but some absorption appears to be missing in the two smallest passbands, about 40% in the 2×1.5Å band and about 60% in the 2×0.75Å passband, indicating that the planetary absorption is partially being resolved out. We modelled this by measuring the absorbed flux as function of passband for a planetary Lorentzian line profile with a width equal, 2× and 4× times the width of the stellar Na D absorption, normalised to the STIS/HST value. These simulations are shown as the dotted lines *a, b, c* in Fig. 5, and indicate that planetary absorption is likely to be about as broad (within a factor of 2) as the stellar absorption. Also presented in Fig. 5 are two measurements from the re-analysis of the HST/STIS data (Sing et al., 2008a;b), within a band pass of 4.4 and 9 Å. The analysis of Sing et al. is fully consistent with our results, but indicates that the Na line profiles may not be Lorentzian on wide scales. Instead they present narrow cores extending over a broader plateau. The observations presented here are not sensitive to absorption on these large spectral scales.

3.2. Comparison with the Na D absorption in HD189733

Recently, Redfield et al. (2008) measured Na D absorption in the transmission spectrum of the other known bright transiting hot Jupiter HD189733b, at a level of 0.067±0.021% in a passband

of 12Å. Note that their in-transit data originate from short observations of eleven different transit events, but in total reach a similar SNR as the data presented in this paper. The detection of Redfield et al. is about a factor of 3 higher than that measured for HD209458b. From their figure 1 we conclude that they have derived the strength of the Na D feature by integrating $\int_{\Delta\lambda} F_{in}/F_{out}$ instead of integrating $\int_{\Delta\lambda} F_{in}/\int_{\Delta\lambda} F_{out}$. This means that their result cannot be directly compared to the results of HD209458b, since it puts much higher weights (>10×) on the pixels in the center of the stellar absorption lines where most planetary absorption is seen. The number of absorbed photons for a ~1% planetary absorption at the stellar line center would be equal to the number of absorbed photons for a ~0.1% planetary absorption at the stellar continuum. By multiplying the data points from their figure 1 by the stellar flux at each wavelength, we estimate that the measured Na D absorption from HD189733b is only a factor ~2 above that measured for HD209458b. This remaining difference however does not mean that the planets have a different Na atmosphere. Physically, these levels of absorption correspond to a variation in the apparent planetary radius of 0.8% (~750 km) for HD209458b, and 1.0% (~780 km) for HD189733b. Hence the results for both planets are actually very similar.

Remarkably, Redfield et al. (2008) find a significant blueshift of their planetary absorption signal, of the order of ~38 km sec^{-1} (corresponding to ~0.75Å). No such shift of the planetary absorption is present in the transmission spectrum of HD209458b. If this velocity shift is real, it is rather puzzling how it could be produced, since it is about an order of magnitude higher than the expected sound speed in the upper layer of the planet's atmosphere (Brown 2001). We note that the data analysis of Redfield et al. is affected by the intrinsic variations in stellar line shapes due to the Rossiter-McLaughlin effect, due to the use of the $\int_{\Delta\lambda} F_{in}/F_{out}$ integral, which does not have to integrate down to zero, even if there is no additional planetary absorption (see section 2). If the spectra are not evenly distributed over the transit, this can also lead to spurious velocity offsets, although it is difficult to see how these could become larger than the $v\sin i$ of the star.

4. Conclusions

We present the first ground-based detection of the Na D absorption feature in the transmission spectrum of the extrasolar planet HD209458b, fully consistent with the HST measurements by Charbonneau et al. (2002). The absorption is measured at a level of 0.135±0.017%, 0.070±0.011%, and 0.056±0.007% in three passbands of 2×0.75Å, 2×1.5Å, and 2×3.0Å wide, indicating that the absorption is partially resolved out in the two smallest bands. Crucial in our analysis was the removal of an empirical correlation between line depth and the continuum count level in the spectra, likely to be caused by non-linearity of the CCD. We show that due to either changes in the spectral resolution, or intrinsic changes in the stellar line profiles during the transit due to the Rossiter-McLaughlin effect, it is crucial to integrate the atmospheric absorption over a wide-enough passband to avoid spurious effects.

References

Baba, H., et al. 2002, ADASS XI, eds. D. A. Bohlender, D. Durand, & T. H. Handley, ASP Conference Series, Vol.281, 298
Ballester, G. E., Sing, D. K., & Herbert, F. 2007, Nature, 445, 511
Brown, T. M. 2001, ApJ, 553, 1006
Brown, T. M., Charbonneau, D., Gilliland, R. L., Noyes, R. W., & Burrows, A. 2001, ApJ, 552, 699
Charbonneau D., Brown T.M., Noyes R.W., Gilligand R.L., 2002, ApJ 568, 377
Charbonneau D., Allen L., Megeath S., Torres G., Alonso R., Brown T., Gilliland R., Latham D., Mandushev G., O'Donovan F., Sozzetti A., 2005, ApJ, 626, 523
Deming, D., Seager, S., Richardson, L. J., & Harrington, J. 2005, Nature, 434, 740
Ehrenreich, D., Hébrard, G., Lecavelier des Etangs, A., Sing, D. K., Désert, J.-M., Bouchy, F., Ferlet, R., & Vidal-Madjar, A. 2007, ApJ, 668, L179
Knutson, H. A., et al. 2007, Nature, 447, 183
Lundstrom, I., Ardeberg, A., Maurice, E., & Lindgren, H. 1991, A&AS, 91, 199
Moutou, C., Coustenis, A., Schneider, J., St Gilles, R., Mayor, M., Queloz, D., & Kaufer, A. 2001, A&A, 371, 260
Narita, N., et al. 2005, PASJ, 57, 471 (NAR05)
Noguchi, K., et al. 2002, PASJ, 54, 855
Redfield, S., Endl, M., Cochran, W. D., & Koesterke, L. 2008, ApJ, 673, L87
Rossiter, R. A. 1924, ApJ, 60, 15
Seager, S., & Sasselov, D. D. 2000, ApJ, 537, 916
Sing et al. 2008a, ApJ submitted (arXiv:0802.3864)
Sing et al. 2008b, ApJ submitted (arXiv:0803.1054)
Snellen, I. A. G. 2004, MNRAS, 353, L1
Swain, M. R., Vasisht, G., & Tinetti, G. 2008, Nature, 452, 329
Tinetti, G., et al. 2007, Nature, 448, 169
Vidal-Madjar, A., Lecavelier des Etangs, A., Désert, J.-M., Ballester, G. E., Ferlet, R., Hébrard, G., & Mayor, M. 2003, Nature, 422, 143
Vidal-Madjar, A., et al. 2004, ApJ, 604, L69
Winn, J. N., Suto, Y., Turner, E. L., Narita, N., Frye, B. L., Aoki, W., Sato, B., & Yamada, T. 2004, PASJ, 56, 655